International Journal of Modern Manufacturing Technologies
ISSN 2067–3604, Vol. VI, No. 1 / 2014

MODELLING THE CORRELATION BETWEEN FERRITE NUMBER WELD MICROSTRUCTURE OF CRYOGENICS AND DUPLEX STAINLESS STEELS AND CHEMICAL COMPOSITION BY NEURAL NETWORKS

Bormambet Melat[1], Zăgan Sabina[2], Chiţu Greti[1] & Zăgan Remus[2]

[1]"Ovidius" University of Constanta, Faculty of Mechanical Enginering, Blvd. Mamaia, No. 124, 900527, Constanta, Romania
[2] Maritime University of Constanta, Faculty of Naval Electromechanics, Mircea cel Bătrân Street, No. 104, Constanta, Romania

Corresponding author: Zăgan Remus, zagan.remus@gmail.com

Abstract: In this paper, the MATLAB with Artificial Neural Networks toolbox is used for an artificial neural networks was developed to predict ferrite number (FN) of weld microstructure of X6CrNiTi18-10 and different duplex stainless steel. Different modeling method based on artificial neural networks is used by many researchers for a wide range of engineering applications. Ferrite is known to be very effective in reducing the tendency to hot cracking shown by welds in austenitic stainless steels. The strong influence of FN on cryogenic toughness dictates the use of an accurate method for predicting FN in the new high-nitrogen and manganese stainless steel electrodes. Different researchers suggest some models to predict ferrite number using neural networks, but these models need to be extended. We propose a model with two hidden layers feed forward type of artificial neural networks for predict microhardness. In our study we develop a new relation to predict the ferrite number and for the chemical composition provided by the database we calculated also the (Cr_{eq} +Ni_{eq}) and (Cr_{eq} /Ni_{eq}) values for each sample and introduced in the new relation in order to obtain a predicted FN value. As input in our neural networks, we consider the chemical composition and Cr in solution of different welding probe of the cryogenics and different duplex stainless steels. For our purpose we consider more de 90 different data were gathered from experimental results. We consider different format of input parameters that cover the chemical composition and Charpy impact energy and output parameter which is ferrite number. The networks was trained to predict the ferrite number values as output.The artificial neural networs was developed and training using a back propagation algorithm applied to the experimental data from literature. In our study, the back propagation training algorithm has been used in feed forward for hidden layers of our artificial neural networks architecture. Back propagation algorithm, is one of the most used training algorithms for the multilayer perceptron, is a gradient descent technique to minimize the error for particular training pattern in which it adjust the weights. The assignment of initial weights and other related parameters may also influence the performance of the artificial neural network. We consider two different models for neural networks architecture, and the performance of them will be tested. All of the results obtained from experimental studies and predicted by using the training, testing and validation results for two different neural networks architecture will be given. We optimized the neural network architecture to find the best equation to predict microhardness values by specific inputs. The predicted values are in very good agreement with the measured ones.

Key words: Artificial network, Thermal treatments, X6CrNiTi18-10, Microstructures.

1. INTRODUCTION

The industrial usage of steels at low temperatures leads to different studies which tend to increase the installation capacity and security in this field. Cryogenic steels can be used in aeronautic, food, chemical, petrochemical and transportation industries to manufacture equipments, claddings, and pipes and also to joint them by welding in order to obtain, stock and transport fluids which reach low temperatures while using them. Steels and additional materials which must correspond to an accumulated operating time are required taking into consideration their chemical composition and mechanical features such as high failure stress associated with a good tenacity, a bigger fatigue limit, a good weldability, etc. Our scope is to obtain crystalline structures closer to the perfect ones, the control of dislocations density and their displacement, the allying with elements which form substitution solid solutions, the grain sizes increase. The main alloying element in cryogenic steels is Ni because it manifests a strong positive influence on the fragility threshold, 6%Ni lowering the transition temperature at -200 C, the resilience is excellent and the plasticity is high. In many cases, physical, chemical, mechanical and technological properties of metallic materials depend on the applied thermal treatments (reanneal treatment, annealing treatment, hardening, slackening); for austenitic

stainless steels the applied thermal treatments give a better corrosion resistance.
Industrial steels applications at low temperatures lead to different studies that tend to increase both the capacity and safety of the equipment in this field. According to the exploitation temperature and utilization conditions, cryogenic materials can be classified as: Al, Cu, Ni, Ti, Li, Mg, etc. non-ferrous alloys; cryogenic irons; Ni steels; Cr-Ni austenitic steels. Out of the many steels specially made for low temperature application, the optimal steel brand is chosen after a detailed study of its utilization and mechanical properties.

2. MICROSTRUCTURE OF WELD DEPOSITS AND FERRITE NUMBER (FN)

The microstructures of stainless steel weld metal strongly affects weld metal properties, such as mechanical properties, corrosion properties and prediction of weld metal microstructures is therefore a key aspect of stainless steel applications. Duplex stainless steel welds deposits having Cr_{eq} / Ni_{eq} ratio higher than 1.95 solidify completely as ferrite (Chakrabarti, 2013).
Often in welding procedure qualifications is necessarily to know whether a bend test can be passed because the ability to pass a bend test is very important. Most of duplex stainlees steel to pass the bend test must contains in microstructures much ferrite, and less martensite.
Ferrite is known to be very effective in reducing the tendency to hot cracking shown by welds in austenitic stainless steels.
Ferrite measurement techniques evolved after the realization that austenitic stainless steel weld metals, containing a moderate amount of ferrite, were free of hot cracking related weld defects. Ferrite measurement was immediately identified as a method by which engineers could quantify the amount of weld metal ferrite and ensure that their fabrications would be free from hot cracking. The advent of duplex stainless steels further re-emphasized the need for adequate ferrite measurement techniques as a suitable ferrite/austenite phase balance provides adequate mechanical properties and improved corrosion performance (Lundin, 1999).
The hardness values were examined for the as-weld metal and the three different termomechanicaly treatments.
At higher temperatures, the austenitic stainless steel weld metal containing high chromium content tends to undergo a phase transformation of $\delta \rightarrow \gamma + \sigma$, where typically σ is FeCr and γ is austenite (Bormambet, 2011).
The hardness increased with an increasing Cr/Ni equivalent ratio and increasing δ-ferrite content.
Stainless steel 304 often forms some martensite during bending, but bends successfully. If, on the other hand, the weld deposits conteinds appreciable martensite before bending, it probably fail the bend test (Kotecki, 1999).
Usually it is very important that a concentration of 0.03% C or less ensure very low carbon martensite that can pass the bend test.
Ferrite content is expressed either as a percentage or as a ferrite number (FN). This latter approach is often preferred. Ferrite numbers are normally calculated using either DeLong diagram or WRC-1992 diagrams.
Many researchers have been made try to accurately predict the ferrite content in stainless steels, proposing various diagrams that convert the alloy composition into factors, a chromium equivalent (Cr_{eq}) and a nickel equivalent (Ni_{eq}).
To improve the accuracy of ferrite number (FN) prediction in stainless steel weld metal, Siewert proposed a new diagram using a database containing more than 950 alloy compositions from worldwide sources. The diagram is more accurate than the Schaeffler diagram for duplex stainless steel alloys and ferrite contents to 100 FN (Siewert and McCowan, 1988).

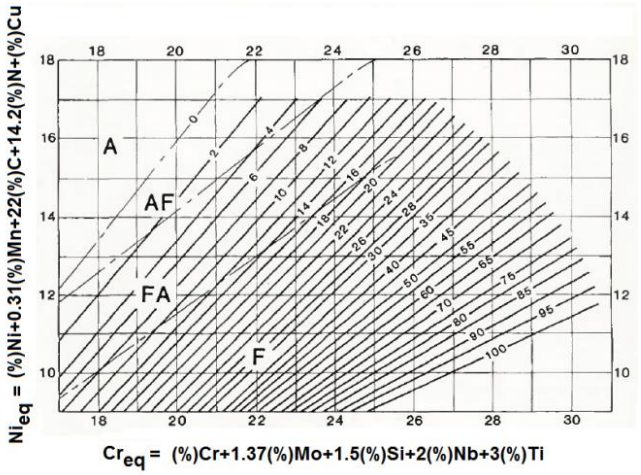

Fig. 1 Diagram DeLong modified proposed by McCowan and Siewert (Siewert, 1988)

The WRC – 1992 diagram modify by Kotecki shown in figure 2 was from the Welding Research Council in 1992. It was modified from the WRC 1988 diagram of McCowan and Siewert by adding to the nickel equivalent coefficient for copper and showing how the axes could be extended to make Schaffler like calculation for dissimilar metal joining.
A duplex stainless steel weld typically has a ferrite content of 25 to 65 FN in according to WRC – 1992 diagram. The increased yield and tensile strength this gives are highly benefial.
There is various versions of constitution diagrams differ primarily in the coefficients that are used to

convert the alloy composition into the Cr_{eq} and Ni_{eq}. An extensive review is given by Bermejo study (Bermejo, 2012).

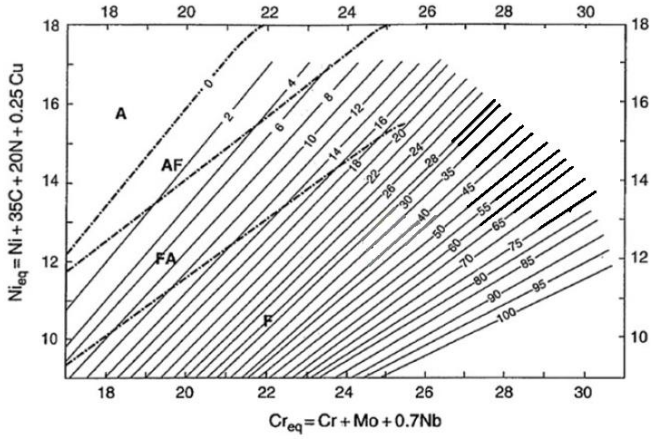

Fig. 2 Diagram WRC – 1992 proposed by Kotecki (Kotecki, 1999)

The ferrite number (FN) calculated from the cladding compositions using WRC-1992 diagram agrees reasonably well with the measured FN. The equations for Cr_{eq} and Ni_{eq} are:

$$Cr_{eq}=Cr+Mo+0.7Nb \quad (1)$$

$$Ni_{eq}=Ni+35C+20N+0.25Cu \quad (2)$$

where the elemental symbols represent the weight percent of each element.
The ferrite number decreases with the rise in heat input and dilution and also decreases with a rise in welding current and welding speed and increases with a decrese in welding gun angle and rise in contact tip to work piece distance (Kannan, 2006).
In his paper Martorano made a study for nineteen different versions of practical methods were formed using Schaeffler, DeLong, and Siewert diagrams and the nickel and chromium equivalent indexes suggested by several authors and showing that the Siewert diagram, including its equivalent indexes gives the lowest relative errors between calculated and measured delta ferrite fractions. (Martorano, 2012).
Vitek use neural network to applied to the problem of predicting ferrite number and develop a new network model, considering the alloy chemical composition as input data (Vitek, 2000).
In our research we use for more than 80 date of cryogenic steels of weldments composition similar with X6TiNiCr18-10 and few date of ferritic stainless steels of weldments.
With the help of the Siewert diagram, figure 2, we evaluate the ferrite number FN for every chemical composition and using the Hammar and Svensson's equations to compute Cr_{eq} and Ni_{eq}, given by relations (3) and (4) for all materials.

$$Cr_{eq}=Cr+1.37Mo+1.5Si+2Nb+3Ti \quad (3)$$

$$Ni_{eq}=Ni+0.31Mn+22C+14.2N+Cu \quad (4)$$

where the elemental symbols represent the weight percent of each element.
For our study we use the new proposed relation for compute ferrite number (FN) for stainless steels weldments, given by:

$$FN=70.9455-182.057(Cr_{eq}+Ni_{eq})+[-157.4284+ +304.906(Cr_{eq}+Ni_{eq})](Cr_{eq}/Ni_{eq})+[74.131- 114.37(Cr_{eq}+Ni_{eq})](Cr_{eq}/Ni_{eq})^2 \quad (5)$$

where Cr_{eq} and Ni_{eq} are given by relations (3) and (4).
For the chemical composition provided by the database we calculated also the (Cr_{eq} +Ni_{eq}) and (Cr_{eq} /Ni_{eq}) values for each sample and introduced in equation 5 in order to obtain a predicted FN value.
The predicted FN values were then compared with the experimental FN provided by the database.

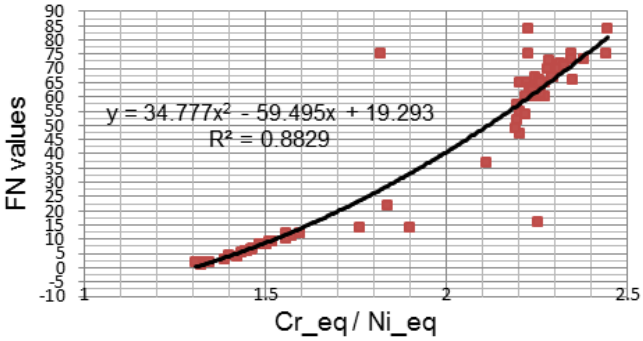

Fig 3. Variation of FN versus Cr_{eq} /Ni_{eq} for 30%< Cr_{eq}+Ni_{eq} <40%

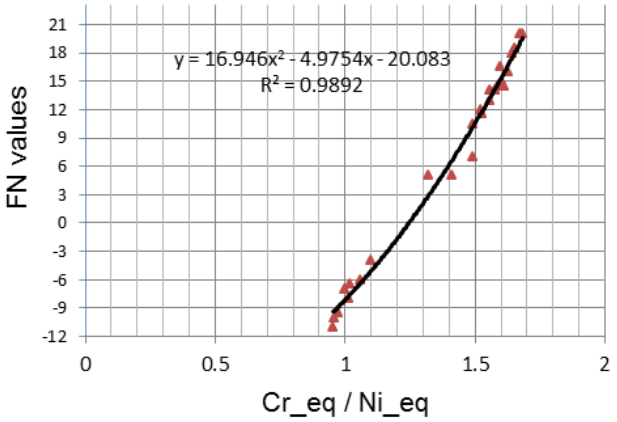

Fig 4. Variation of FN versus Cr_{eq} /Ni_{eq} for 40%<Cr_{eq}+Ni_{eq}<45%

The general expression (5) provides FN estimation with an error of -7.2 FN + 7.1 FN for 1.2<Cr_{eq}/Ni_{eq}<2.44 and 30%<Cr_{eq}+Ni_{eq}<40%.

The general expression (5) provides FN estimation with an error of -4.01 FN + 1.48 FN for 0.9< Cr_{eq}/Ni_{eq} <1.68 and 40%< Cr_{eq}/Ni_{eq} <45% .
The cryogenic toughness of type X4CrNiMoN18-10, X6CrNiTi18-10, 308L, 309 and 316L stainless steel welds is determined by the interrelated and sometimes opposing effects of the individual alloying elements and (FN) the ferrite number (Mori, 1985). The FN has been found to be the dominant factor in determining CVN toughness in these materials, (McCowan, 1987).

3. ARTIFICIAL NEURAL NETWORK THEORY

Neural networks find their origin in biological science. However, the basis of that has been extended to artificial neural networks, which is the general terminology used to describe the mathematical models.
McCulloch and Pitts (McCulloch and Pitts, 1943) defined artificial neurons for the first time and developed a neuron model.
In 1958 Frank Rosenblatt, an American psychologist, proposed the perceptron, a more general computational model than McCulloch–Pitts units (Rojas, 1996). The essential innovation was the introduction of numerical weights and a special interconnection pattern. In the original Rosenblatt model the computing units are threshold elements and the connectivity is determined stochastically. Learning takes place by adapting the weights of the network with a numerical algorithm. Rosenblatt's model was refined and perfected in the 1960s and its computational properties were carefully analyzed by Minsky and Papert (Minsky and Papert, 1969). McCulloch and Pitts' network formed the basis for almost all later neural network models, figure 5.
Their adaptive nature is a very important feature of these networks, where "learning by example" replaces "programming" in solving problems. This feature makes such computational models very appealing in application domains where one has little or incomplete understanding of the problem to be solved but where training data is readily available (Somkuwar, 2012).
The basis of a neural network is shown in figure 1 is composed of five main parts: the inputs x_i in the first layer of neurons, weights W_{ij} accepted by each neuron, sum function, activation function (purelin function, log-sigmoid or tangential function) and the outputs O_j.
Inputs are information that enters the neuron from other neurons of from external world. Weights are values that express the outcome of an input set or another process element in the preceding layer on this process element. Sum function is a function that calculates the effect of inputs and weights completely on this process element.

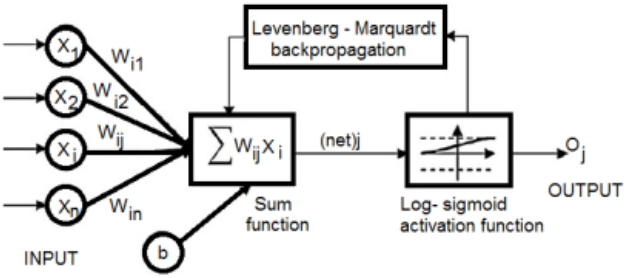

Fig. 5. Architecture of neural network (Ince, 2004)

This function computes the net input that approaches a neuron (Beale et al., 2013). The weighted sums of the input components (net)j are calculated using the below equation as follows:

$$(net)_j=\sum W_{ij}x_i+b \qquad (6)$$

where $(net)_j$ is the weighted sum of the jth neuron for the input received from the preceding layer with n neurons, W_{ij} are the interconnections weights between the jth neuron in the previous layer, x_i is the output of the ith neuron in the previous layer (Beale et al., 2013), b represent the bias for the neuron and have a fix value as internal addition.
Activation function is a function that processes the net input obtained from sum function and determines the neuron output.
In general for multilayer feed-forward models as the activation function, sigmoid activation function is used. The output of the jth neuron $(out)_j$ is computed using equation (6) with a sigmoid activation function as follows (Hopfield, 1982).

$$O_j=f(net)_j=1/(1+e^{-\alpha(net)_j}) \qquad (7)$$

where α is constant used to control the slope of the semilinear region. The sigmoid nonlinearity activates in every layer except in the input layer (Beale et al., 2013). The sigmoid activation function represented by Eq. (7) gives outputs in (0, 1).
Neural networks consist of a large class of different architectures. The most useful neural networks in function approximation are Multilayer Layer Perceptron (MLP) and Radial Basis Function (RBF) networks.
A typical architecture of a multilayer perceptron neural network is composed of the following components:
-one input layer that receives signal from the environment
-one or more outputs layer that conveys the signals to the environment
-one or more hidden layers that keep some input and output signals within the network itself.

Table 1 The range of the input and the output parameters in ANN model

Parameters	Minimum	Maximimum	Mean	Standard deviation
Input				
C (wt%)	0.013	0.127	0.049051	0.021805
Si (wt%)	0.29	0.92	0.625515	0.122182
Mn (wt%)	0.82	7.82	1.791703	1.650183
P (wt%)	0	0.28	0.022444	0.034944
S (wt%)	0	0.054	0.01261	0.015133
Al (wt%)	0	0.068	0.000687	0.006834
Ti (wt%)	0	0.038	0.001937	0.007644
V (wt%)	0	0.187	0.005293	0.022296
Cu (wt%)	0	0.41	0.038444	0.073814
Ni (wt%)	7.46	16.66	11.83459	3.037399
Cr (wt%)	16.05	25.1	21.21382	2.193021
Mo (wt%)	0	3.28	1.477515	1.430535
Nb (wt%)	0	0.056	0.010323	0.015282
N (wt%)	0	0.016	0.057283	0.063633
W (wt%)	0	0.085	0.000859	0.008543
Co (wt%)	0	0.24	0.004848	0.33938
Output				
FN	-11.5	84		

Figure 6 shows a typical architecture of a multilayer perceptron neural network with an input layer, two hidden layers and one output layer.

Many algorithms exist for determining the network parameters. In neural network literature the algorithms are called *learning* or *teaching* algorithms, in system identification they belong to *parameter estimation* algorithms. The most well-known are back-propagation and Levenberg-Marquardt algorithms.

Backpropagation algorithm, one of the most well-known training algorithms for the multilayer perceptron, is a gradient descent technique to minimize the error for a particular training pattern in which it adjusts the weights by a small amount at a time (Rojas, 1996). For small- and medium-sized networks and patterns, the Levenberg–Marquardt algorithm is remarkably efficient and strongly recommended for neural network training (Yu and Wilamowski, 2011).

The procedure of teaching algorithms for multilayer perceptron networks consist in:

a. Defined the structure of the network. In the network, it is necessarily to choose activation functions and to initialize weights and biases.

b. We define the parameters associated with the training algorithm like error goal, maximum number of epochs.

c. Call the training algorithm.

d. At the end when the neural network has been determined, the result is first tested by simulating the output of the neural network with the measured input data. This is compared with the measured outputs.

Final validation must be carried out with independent data.

4. DATA COLLECTION

The measurements were performed on the cryogenic steel sample X6CrNiTi18-10 or AISI 321, welded.

The chemical composition %: C-0.034,Si-0.69,Mn-1.70, Cr-18.55, Ni-9.41, Mo-0.28, Cu-0.35,Ti-0.0018, Nb-0.049, Al-0.068, W-0.085, V-0.061, Co-0.24

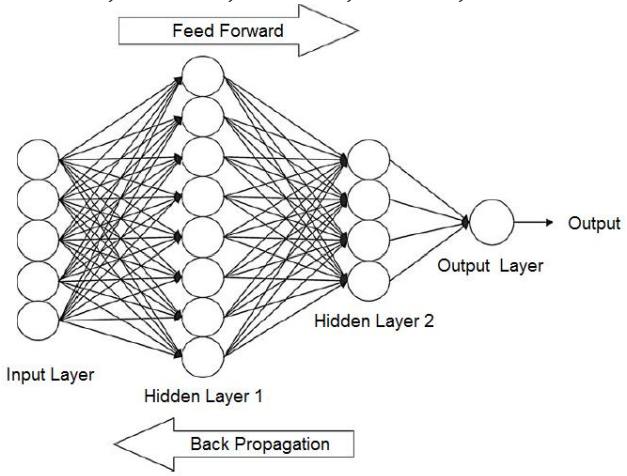

Fig. 6. The architecture of multilayer percepton neural network (Nazari, 2012)

Fig. 7. Cryogenic sample used

Photomicrographs of the stainless steel specimen in base material (see fig. 7a) and in Heat-Affected-Zone (see fig. 7b) emphasize that the structure has a dendrite aspect compound of austenite + ferrite.

The ultrasonic testing of the cryogenic material X6TiNiCr180 was made in the base material and in the weld without being exposed to a thermal treatment (sample). After that, the material was exposed to two thermal treatments: welding + hardening (different samples) and then welding + hardening + annealing treatment (different samples). Metallographic tests which emphasize the grains and their changes due to the thermal treatment to which they are submitted were mare for all the three samples. It was noticed the existence of chromium carbide in the base material and in the weld. The frequency spectrum of the ultrasonic response obtained by PSD (Power Spectral Density) shows a

prevalent austenitic structure in the base material and in the weld prevails a structure compounds of austenite + ferrite + chromium carbide (Zăgan and Petculescu, 2007).

a) b) c)

Fig. 8 The metallographic microstructure X6CrNiTi18-10
a) base material; b) HAZ; c) limits of phases

In the present investigation, the artificial neural network has been trained, tested and validated for prediction ferrite number (FN). For this purpose, the experimental data consist in chemical composition of cryogenic stainless steels and their weldments, for our propes and supplementary we use date from literature, like X4CrNiMoN18-10 (Deimel, 1998), AISI316L (Jang and Lee, 2012), 316L (Naumann et al., 2012), AISI309 (Brooks and Lambert, 1979), and few data of duplex stainless steel IS2062 (Chakrabarti et al., 2013), (Kannan and Murgon, 2006), 17.5Cr16.5Ni welds (Matsumoto et al., 1987).
The input variables of the ANN modeling are the weight percent of alloying elements.
These parameters along with their range have been summarized in Table 1.

5. ANN MODEL CONSTRUCTION

Two ANN modeled in this research. The input layers have sixteen neurons for every ANN model and the parameters are given in table 2 and 3.

Table 2. The Neural Networks values used in ANN model 1

Parameters	ANN
Number of input layer units	16
Number of hiden layers	2
Number of first hidden layer units	10
Number of second hidden layer units	5
Number of output layer units	1

The values for input layers were carbon weight percent (C), silicon weight percent (Si), manganese weight percent (Mn), phosphorous weight percent (P), sulfur weight percent (S), aluminum weight percent (Al), titanium weight percent (Ti), vanadium weight percent (V), copper weight percent (Cu), nickel weight percent (Ni), chromium weight percent (Cr), molybdenum weight percent (Mo), niobium weight percent (Nb), nitrogen weight percent (N), tungsten weight percent (W) and cobalt weight percent (Co).

The neurons of neighboring layers are completely interconnected by weights. Finally, the output layer neurons produce the network prediction as a result.
From the total 90 gathered date, 60 were randomly selected and trained by the network, 30 data were used for validation and the other 30 data were used for testing the network. In this study, the back-propagation training algorithm has been utilized in one feed-forward hidden layer.

Table 3. The Neural Networks values used in ANN model 2

Parameters	ANN
Number of input layer units	16
Number of hiden layers	2
Number of first hidden layer units	14
Number of second hidden layer units	7
Number of output layer units	1

The nonlinear sigmoid activation function was used in each the hidden layer and purelin in the neuron outputs at the output layer. The trained model was only tested with the input values, and the predicted results were close to experiment results.

6. RESULTS AND DISCUSSION

6.1 ANN Modeling with MATLAB

Back-propagation multilayer feedforward ANNs (ANN-1 and ANN-2) were created using the Neural Network Toolbox in Matlab 7 package. ANN-1 comprise the input layer, two hidden layer and the output layer, see Figure 9.

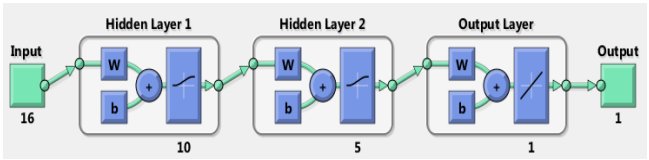

Fig. 9. The ANN-1 model used in MATLAB

Also ANN-2 comprise the input layer, two hidden layer and the output layer, see and Figure 10.

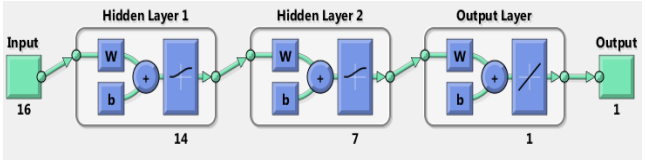

Fig. 10. The ANN-2 model used in MATLAB

6.2 Training and Validation

The ANNs are trained by introducing a set of examples of proper network behaviour to the ANNs. During training, the learning rule is used to iteratively

adjust the weights and biases of the network in order to move the network outputs closer to the target values by minimizing the network performance indicator. The Levenberg-Marquardt training algorithm, which has a higher rate of convergence, is used for the training of both ANN-1 and ANN-2.
Figure 11 presents the comparison between measured and predicted results for ferrite number of stainless steels weldments.
We consider that this approach can be very useful in modeling the mechanical properties of naval steels, because there is a concordance between the predicted and measured values indicated. The prediction values match the measured amounts very well. This clearly indicates the accurate function of the trained ANN-2 in predicting the ferrite number values.
In Figure 11a, b and c, we present the training, validation and testing predicted ferrite number values results of ANN-2 model, and these results are obtained from experimental studies.

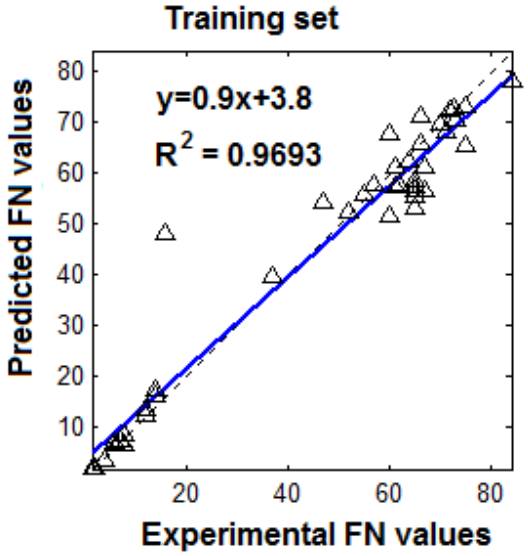

(a)

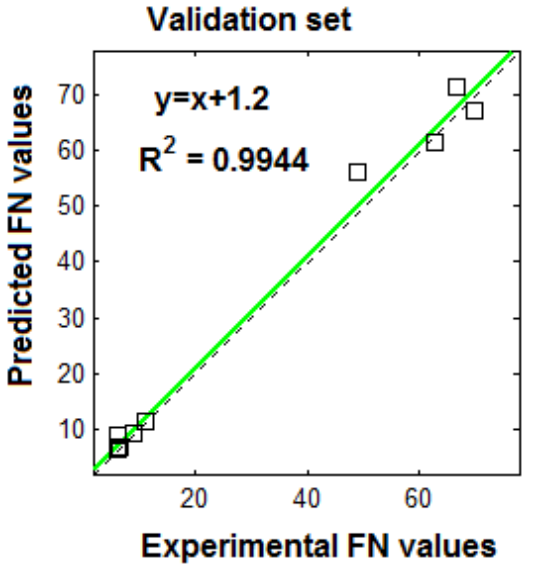

(b)

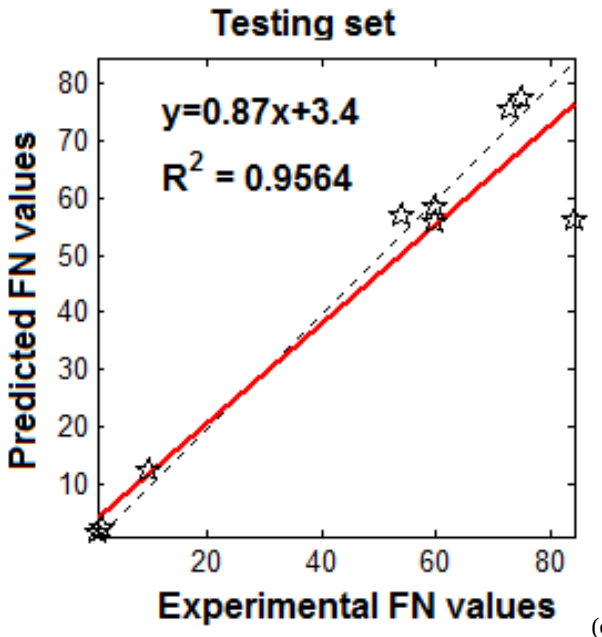

(c)

Fig. 11. Correlation of the measured and predicted ferrite number values in (a) training, (b) validation and (c) testing sets for ANN model 2

The linear least-square fit line, its equation and the R^2 values are shown also in these figures for the training, validation and testing data.
It can see in Figure 11, the values obtained from the training, validation and testing in ANN-2 model are very close to the experimental FN data results. Also the result of testing phase in Figure 11 shows that the ANN-2 model are capable of generalizing between input and output variables with reasonably good predictions. The best value of R^2 is 99.44 % for validation set in the ANN-2 model.
All of R^2 values show that the proposed ANN-2 model are suitable and can predict ferrite number values very close to the experimental values.

7. CONCLUSIONS

For determination the ferrite content in stainless steel weld deposits we propose a general relation (5). Some times the weld deposit is not available such as in new projects where alternative welding consumables are being considered or simply when it is necessary only to get an approximate value, then predictive methods such diagrams WRC – 1992, or different modified and also the proposed model for ferritic and austenitic stainless steels have their scope. Two artificial neural network models (ANN-1 and ANN-2) was developed to predict the ferrite number values of stainless steels weldments. The values predicted in the presented models are in very good agreement with those measured by experimental results, and computed respectivelly.

8. REFERENCES

1. Anderson, T.L., McHenry, H.I., (1982), *Fracture toughness of steel weldments for artic structures*, National Measurement Laboratory, Colorado.

2. Baek, J.H., Kim, Y.P., Kim, W.S., Kho Y.T., (2002), *Effect of temperature on the Charpy impact and CTOD values of type 304 stainless steel pipeline for LNG transmission*, KSME International Journal, 16(8), pp 1064-1071.

3. Beale, M.H., Hagan, M.T., Demuth, H.B., (2013), *Neural Network Toolbox™. User's Guide*, The Mathworks Inc., www.mathworks.com.

4. Bermejo, M.A.V., (2012), Predictive measurement methods for delta ferrite determination in stainless steels, Welding Journal, 91, pp.113-s – 121-s.

5. Bormambet M., Zăgan R., (2011), *Experimental studies on the influence of deep hardening treatment on the welded joints of cryogenics steels*, Proceedings of the 15th International Conference MODTECH 2011: NEW FACE OF TMCR, Vadu lui Voda, Chişinău, Republic of Moldova, Mai, ISSN 2066-3919, pp. 113-116.

6. Bormambet, M., Zăgan, R., (2012), *Nondestructive and destructive experimental research of welded joints of steels used at low temperatures*, Metalurgia International, XVII(9), pp.85-90;.

7. Brooks J.A., Lambert jr, F.J., (1978), *The effects of phosphorus, sulfur and ferrite content on weld cracking of type 309 stainless steel*, Welding Research Supplement, pp. 139-s - 143-s.

8. Chakrabarti B., Das H., Pal T.K., (2013), *Effect of process parameters on clad quality of duplex stainless steel using GMAW process*, trans Indian Inst Met, 66 (3), pp. 221-230.

9. David, S.A., (1981), *Ferrite morphology and variations in ferrite content in austenitic stainless steel welds*, Welding research Supplement, pp. 63-s -70-s.

10. Deimel, P., Fischer, H., Hoffmann, M., (1998), *Strength and toughness properties of two nitrogen alloyed stainless steels and their submerged arc weldments at cryogenic temperatures*, Journal of Materials Science, 33 , pp. 1105-1116.

11. Hammar, Ö., and Svensson, U., (1979), *Influence of steel composition on segregation and microstructure during solidification of austenitic stainless steels*, International Conference on Solidification and Casting of Metals, Sheffield, UK. The Metals Society, pp. 401–410.

12. Hopfield, J.J., (1982), *Neural networks and physical systems with emergent collective computational abilities*, Proc Nat Acad Sci, 79, pp. 2554–2558.

13. Ince R., (2004), *Prediction of fracture parameters of concrete by artificial neural networks*, Journal of Engineering Fracture Mechanics, 71 (15), pp. 2143-2159.

14. Jang, A.Y., Lee, H.W., (2012), *Influence of sigma phase on pitting resistance depending on solidification mode in AISI316L weld metal*, Metallurgical and Materials Transactions A, 43A, pp. 1736-1741.

15. Kane, F.,S., Farland, T.,A., Siewert, T.,A., McCowan, C., N., (1999), *Welding consumable development for a cryogenic (4K) application*, Welding Research Supplement, pp.292-300.

16. Kane, S., (1992), *Fracture toughness requirements for RHIC cryogenic design*, RHIC project, Brookhaven National Laboratory.

17. Kannan, T., Murugan, N., (2006), *Prediction of ferrite number of duplex stainless steel clad metals using RSM (response surface methodology)*, Welding Research Supplement, pp. 91-100.

18. Kotecki, D.J., (1999), *A martensite boundary on the WRC – 1992 diagram*, Welding Research Supplement, pp.180-192.

19. Khalaj., G., Yoozbashizadeh, H., Khodabandeh, A., Nazari, A., (2011), *Artificial neural networks to predict the effect of heat treatments on Vickers microhardnes of low carbon Nb microalloyed steels*, Neural Comput & Applic., doi:10.1007/s00521-011-0779-z.

20. Khalaj, G., Nazari, A., Yoozbashizadeh, H., Khodabandeh, A., Jahazi, M., (2012), *ANN model to predict the effects of composition and heat treatment parameters on transformation start temperature of microalloyed steels*, Neural Comput & Applic., doi:10.1007/s00521-012-1123-6.

21. Khalaj, G., Khoeini, M., Khakian-Qomi, M., (2012), *ANN-based prediction of ferrite fraction in continuous cooling of microalloyed steels*, Neural Comput Appl. doi:10.1007/s00521-012-0992-4

22. Lacombe, P., Baroux, B., Beranger, G., (1993), *Stainless Steels*, Les Editions de Physique Les Ulis, pp. 549-591.

23. Lightfoot, M.P., Bruce, G.J., McPherson, N.A., Woods, K., (2005), *The application of artificial neural networks to weld induced deformation in ship plate*, Supplement to the Welding Journal, February 2005, pp.23-30.

24. Lundin, C.D., Ruprecht, W., Zhou, G., (1999), *Literature Review – Ferrite measurement in austenitic and duplex stainless steel castings*, materials joining research group, Department of Materials Science and Engineering, The University of Tennesssee, Knoxville.

25. Martorano, M.A., Tavares, C.F., Padilha, A.F., (2012), *Predicting delta ferrite content in stainless steel castings*, ISIJ International, 52(6), pp. 1054-1065.

26. Matsumoto, T., Satoh, H., Wadayama, Y., Hataya, F., (1987), *Mechanical properties of fully austenitic weld deposits for cryogenic structures*, Welding Research Supplement, pp.120-128.

27. McCowan, N.C., Siewert, T.A., Reed, R.P., Lake, F.B., (1987), *Manganese and Nitrogen in stainless*

steel SMA welds for cryogenic service, Welding Research Supplement, pp.84-92;
28. McCulloch, W. S., Pitts, W., (1943), *A logical calculus of the ideas immanent in neurons activity*, Bull. Math. Biophys., 5, pp. 115–13.
29. Minsky, M., Papert, S., (1969), *Perceptrons: An Introduction to Computational*, Geometry, MIT Press, Cambridge, MA.
30. Mori, T., and Kuroda, T., (1985), *Prediction of energy absorbed in impact for austenitic weld metals at 4.2 K, Cryogenics* 25, pp.243- 248.
31. Naumann, M.T., Mohideen, S.R., Kaleem, N., (2012), *Material characterization of 316L stainless steel after being subjected to cryogenic treatment*, International Journal of Mechanical and Industrial Engineering , 2(1), pp. 44-48.
32. Nazari A., Milani, A.A., Zakeri, M., (2011), *Modeling ductile to brittle transition temperature of functionally graded steels by artificial neural networks*, Comput. Mater. Sci., 50, pp. 2028-2037.
33. Nazari A., (2012), *Modeling the correlation between Charpy impact energy and chemical composition of functionally grade steels by artificial neural networks*, Neural Comp. & Applic., doi: 10.1007/s00521-011-0761-9.
34. Nazari A., (2011), *Application of artificial neural networks for analytical modeling of Charpy impact energy of functionally graded steels*, Neural Comput Appl. doi:10.1007/s00521-011-0761-9.
35. Nazari A, Milani AA, Zakeri M., (2011), *Modeling Ductile to brittle transition temperature of functionally graded steels by artificial neural networks*, Comput Mater Sci 50, pp. 2028–2037.
36. Nazari A (2011), *Microhardness profile prediction of functionally graded steels by artificial neural networks*, Int J Damage Mech. doi:10.1177/1056789511432653.
37. Petculescu, P., Zăgan, R., Bormambet, M., (2007), *The influence of thermal treatments on acoustical-spectral parameters*, Journal of Optoelectronics and Advanced Materials, 9(12), pp.3847-3851.
38. Pickering, F. B., and Gladman, T., (1961), *An investigation into some of the factors which control the strength of carbon steels*. ISI Special Report 81, The Iron and Steel Institute, pp. 10–20.
39. Rojas, R., (1996), *Neural Networks – A systematic introduction*, Springer-Verlag, Berlin, New-York.
40. Siewert, T.A., McCowan, C.N., Olson, D.L., (1988), *Ferrite number prediction to 100 FN in stainless steel weld metal*, Welding Research, pp. 289-298.
41. Szumachowski, E.R., Reid, H.F., (1979), C*ryogenic toughness of SMA austenitic stainless steel weld metals: Part II – Role of nitrogen,* Welding Research Supplement, pp. 34-44.
42. Somkuwar, V., (2012), *Prediction of Mechanical Properties of Steel Using Artificial Neural Network*, International Journal of Engineering, Business and Enterprise Applications (IJEBEA), 3(1), pp. 7–13.
43. Somkuwar, V., (2013), *Prediction of Hardness of High Speed Steel Using Artificial Neural Network*, International Journal of Engineering Science and Innovative Technology (IJESIT), 2(2), pp.93-98.
44. Tugrul O, Yigit K, (2005), *Predictive modeling of surface roughness and tool wear in hard turning using regression and neural networks*, Int J Mach Tools Manuf, 45, pp.467–479.
45. Trzaska J, Dobrzanski LA, (2005), *Application of neural networks for designing the chemical composition of steel with the assumed hardness after cooling from the austenitising temperature*, J Mater Process Technol, 164–165, pp. 1637–1643.
46. Vaynman, S., Fine, M.E., Chung, Y.W., (2009), *Super tough steel for bridges and other applications*, Final report USDOT University Transportation Center, Northwestern University.
47. Vitek, J.M., Iskander Y.S., Oblow E.M., (2000), *Improved ferrite number prediction in stainless steel arc welds using artificial neural networks – Part 1: Neural Networks Development*, Welding research supplement, pp. 33-40.
48. Vitek, J.M., Iskander Y.S., Oblow E.M., (2000), *Improved ferrite number prediction in stainless steel arc welds using artificial neural networks – Part 2: Neural Networks results,* Welding research supplement, pp. 41-50.
49. Zăgan, R., Petculescu, P. (2007), *Ultrasonic spectroscopy of welded cryogenic materials*, Journal of Optoelectronics and Advanced Materials, 9(6), pp.1803-1807.
50. Zăgan R., Petculescu P, Bormambet M., Petculescu A, (2009), *Spectral characterization of W4541 stainless steel, for structural components identification*, Proceedings of the 13th International Conference ModTech - New face of TMCR , *Modern Technologies, Quality and Innovation - New face of TMCR,* Editors Nedelcu D., Slătineanu L., Mazuru S., Editura Politehnium, Iaşi-Chişinău, pp. 699-702.
51. Zăgan R., Petculescu P, Bormambet M., Petculescu A, (2009), *Evaluation of spectral response in the austenitic steel alloy 10TiNiCr180*, Proceedings of the 13th International Conference ModTech, New face of TMCR, *Modern Technologies, Quality and Innovation - New face of TMCR,* Editors Nedelcu D., Slătineanu L., Mazuru S., Editura Politehnium, Iaşi-Chişinău, pp. 703-706.
52. Yu, H., Wilamowski, B. M., (2011), *Industrial Electronics Handbook*, 2nd Edition, 5, Publisher CRC Press, pp. 12-1 to 12-15.

Received: November 1, 2013 / Accepted: June 15, 2014 / Paper available online: June 20, 2014 © International Journal of Modern Manufacturing Technologies.